LONG TERM CLIMATE VARIABILITY OF MERCURY'S POLES. M. A. Siegler[1], B.G. Bills[2], and D.A. Paige[1], [1]UCLA, Department of Earth and Space Sciences, [2]NASA Jet Propulsion Laboratory

Introduction: Since the early 1990's it has been generally accepted that water ice is present in permanently shadowed regions near the poles of Mercury [1, 2]. Radar bright features correspond well with areas modeled to remain below roughly 100K, a temperature at which ice would be stable from surface sublimation for billions of years [3]. However, a conclusive story explaining the presence of ice on Mercury (and the relative lack thereof on the Moon) has yet to be written. The Messenger mission will soon provide an unprecedented look into the polar regions and their near subsurface. In anticipation, we examine some of the long term orbital variations experienced by Mercury and the effects they might have on ice distribution. With future modeling, including Messenger derived topography, these concepts might aid in diagnosing if geographic ice distributions are consistent with the present or past Mercurial climate.

Introduction to Mercury's orbit: Since the 1960's [4] Mercury has been identified to be in an eccentric orbit with a 3:2 spin-orbit resonance. This unique geometry causes noon to occur at perihelion only at 0° and 180° longitude, causing these longitudes to have warmer mean and maximum annual temperatures. Thus, rather than a polar circle, isothermal temperature distributions at the poles of Mercury are better described by an ellipse with the long axis at 90° and 270° longitude.

This ellipse however is not constant over long timescales. The most notable change, and likely the dominant effect on long term climate, is in eccentricity. Shown in Figure 1, now standard secular orbit calculations from Brouwer and Van Woerkom [5] find a Mercury's orbital eccentricity should range from roughly 0.11 to 0.24 over a roughly 10^5 year timescale (with the present eccentricity being 0.206). Recent calculations show early chaotic eccentricities may have increased up to 0.325 [6].

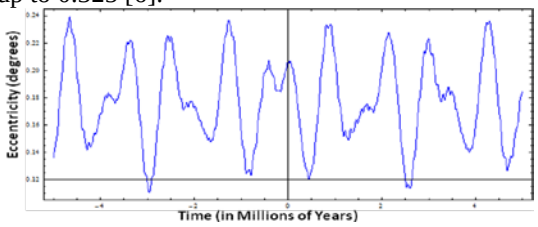

Figure 1: Long term eccentricity of Mercury [5].

The orbital inclination and obliquity can also vary on similar timescales. However, orbital inclination, which ranges between roughly 4 and 11 degrees, will have no direct effect on a planets insolation pattern. Obliquity will impact polar illumination, but Mercury's obliquity typically falls between 2 and 4 minutes of arc for at least the past 10 million years [7]. Higher obliquities may have been possible in the past, but only predating Mercury's capture into its Cassini State [8, 9].

Illumination to temperatures in a crater: One can begin to approach Mercury's climate by looking at yearly average and maximum illumination. Taking account for the 0.386 AU semimajor axis and assuming zero obliquity, equatorial insolation will can be illustrated as in Figure 2, where the blue line represents annual average insolation, the red maximum and the green various snapshots throughout the year.

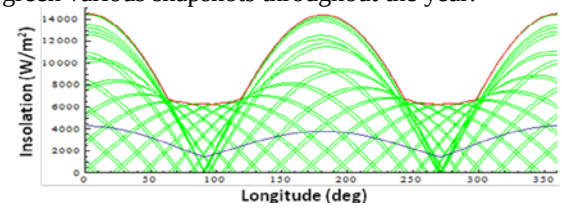

Figure 2: Average (blue) , Maximum (red), and instantaneous (green) insolation at the equator of Mercury.

Maximum and average annual temperatures can be approximated by assuming radiative equilibrium with either the maximum or minimum calculated insolation. Simply assuming $T \approx [Q(1\text{-}A)/(\sigma\varepsilon)]^{1/4}$ where A is the surface albedo (10% here), σ is the Stefan–Boltzmann constant, ε is the surface emissivity (unity here), and Q is either the maximum or mean insolation. This approximation is not applicable for calculating minimum temperatures, but can serve as a good guide in approximation amplitudes during periods where surface thermal properties are less important.

Within a crater, one can approximate temperatures by assuming the crater to be a section of a sphere. This does not imply a hemispherical crater, but rather a slice of a sphere with a given diameter to depth ratio. This approximation works well for craters smaller than roughly 20km, where bowl shaped floor geometries tend to dominate [10]. Assuming a Lambertian surface, the insolation inside such a bowl-shaped crater can be calculated:

$$Q_c = S\frac{4\varepsilon(1-A)}{D^2}\left(1+\frac{A}{\varepsilon}\right)|\cos\gamma|$$

where S is the solar constant (at 0.386 AU) and D is the diameter to depth ratio, and γ is the instantaneous Sun angle [11]. Figures 3-6 assume a diameter to depth ratio of 5.

Geographic extent of ice stability: We can now examine the geographical extent of ice stability for a crater of a given diameter to depth ratio. Figures 3 and 4 show the modeled mean and maximum temperatures at (a) 0.11 and (b) 0.24 eccentricity. Lower eccentrici-

ties will act to circularize the polar isothermal ellipse, higher eccentricities will elongate it.

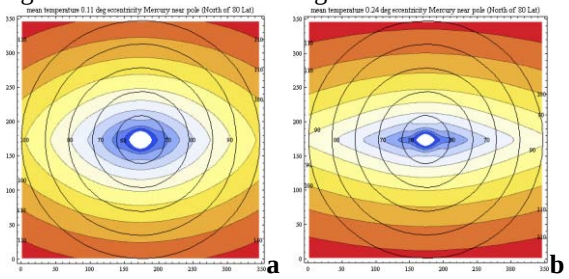

Figure 3: Mean temperatures at (a) 0.11 and (b) 0.24 eccentricity

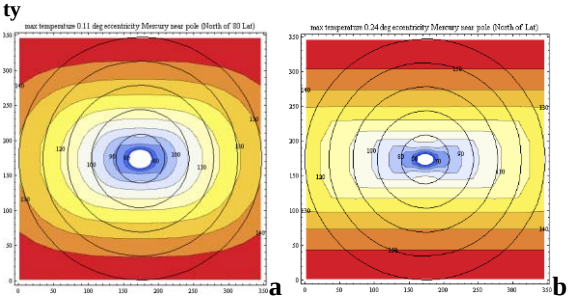

Figure 4: Maximum temperatures at (a) 0.11 and (b) 0.24 eccentricity.

However, identifying the geographical extent of ice stability is a more complex problem than one might first assume. Simply contouring the area with mean temperatures below 100K might seem a logical marker of stability, but does not address maximum temperatures. A full model of ice supply and burial is essential.

Temperature Amplitude: A better estimate might be yearly temperature amplitude. As ice is most mobile for vapor diffusion during warmer parts of the year, looking at mean and maximum temperatures can serve as a reasonable estimate of which longitudes might move ice most efficiently during this warm period. The larger the thermal gradient, the more mobile vapor will be. Thus an area with relatively warm maximum temperatures (100-150K) with a high diurnal amplitude might be better at driving ice down into the subsurface than one in deep freeze (<90K) [11]. Assuming that ice is supplied from above, this "pumping" process might represent the most efficient way to bury ice, given only slow burial and gardening as other means of protection from sublimation and surface loss processes.

Figure 4 illustrates the yearly temperature amplitude at (a) 0.11 and (b) 0.24 eccentricity. Here we see there may be a large change is the geographic extent at which pumping might occur does vary dramatically over Mercury's recent history. During lower eccentricities, the longitudinal extent of areas with large pumping amplitudes increased dramatically. If Messenger's polar data hints at ice having this wider extent, it might serve as an argument that is was "pumped" down at some point in Mercury's semi-distant past. However, if high eccentricity pumping (which better represents the modern environment) drives ice deposition, a relatively narrow longitudinal distribution of ice might argue recent delivery. Likewise, the proposed chaotic 0.325 eccentricity would predict very narrow longitudinal distributions of pumped ice.

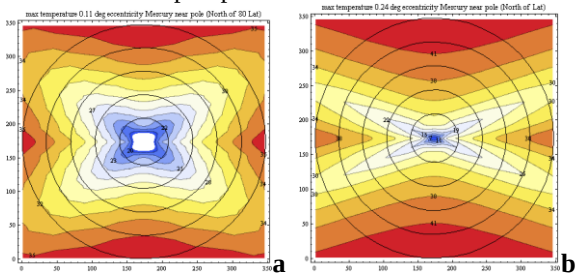

Figure 5: Yearly amplitudes at (a) 0.11 and (b) 0.24 eccentricity.

Long term, deep temperature variation: However, yearly thermal waves will not penetrate more than roughly a meter (assuming Moon-like regolith thermal properties). Mobility of deeper ice, which might feed or be fed by detectable surface reservoirs from below, depends on very long term surface temperature variations. Figure 6a shows the amplitude of these very deep thermal waves assuming a slow transition from 0.11 to 0.24 eccentricity. The highest amplitude waves on the 10^5 year timescale (multi-meter depth) occur along the $90/270^o$ meridian, with relatively modest amplitudes along the "hot" longitudes 0^o and 180^o. Long term pumping cause by the variation of eccentricity could itself allow subsurface ice to be mobile enough to re-bury itself to depths where it can remain stable from upward diffusion.

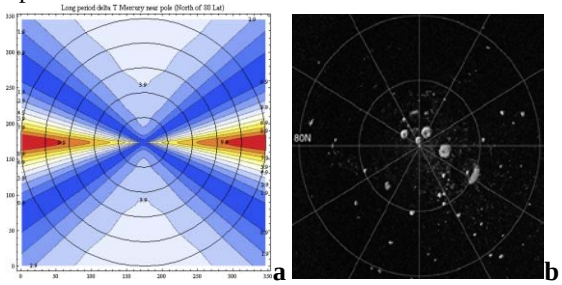

Figure 6: (a) Amplitude of deep thermal waves (10^5 year timescale). (b) North polar radar data from [12].

Conclusions: As seen if Figure 6b, none of these models give anything more than a qualitative match to the distribution of ice as identified by radar observations [12]. However, such simple models can guide study when detailed polar data from the Messenger and BepiColumbo missions become available.

References: [1] Slade 1992 [2] Paige D.A. *et al.* [3] Vasavada et al (1999) [4] Columbo G. (1965) Nature 208, 575 [5] Brouwer, D. & Van Woerkom, A. J. J.(1950) Astron. Pap. Am. Ephem. XIII, part II, 81–107 [6] Correia A.C.M. and Laskar J. (2004) Nature 429, 848-850. [7] Bills B.G. and Comstock R.L. (2005) JRG 110 E04006 [8] Yseboodt and Margot (2006) Icarus 181,2, 327-337 [9] Peale S.J (1974) Astronomical Journal, Vol. 79, 722-744 [10] Pike R.J. (1977) LPSC 8, 3427-3436. [11] Siegler M.A. *et al.* (2011) JGR in press. [12] Harmon *et al.* (2010) Icarus in press.